



HAL
open science

Graph Fourier Transform of fMRI temporal signals based on an averaged structural connectome for the classification of neuroimaging

Abdelbasset Brahim, Nicolas Farrugia

► To cite this version:

Abdelbasset Brahim, Nicolas Farrugia. Graph Fourier Transform of fMRI temporal signals based on an averaged structural connectome for the classification of neuroimaging. 2019. hal-02302538v1

HAL Id: hal-02302538

<https://imt.hal.science/hal-02302538v1>

Preprint submitted on 1 Oct 2019 (v1), last revised 4 Mar 2020 (v2)

HAL is a multi-disciplinary open access archive for the deposit and dissemination of scientific research documents, whether they are published or not. The documents may come from teaching and research institutions in France or abroad, or from public or private research centers.

L'archive ouverte pluridisciplinaire **HAL**, est destinée au dépôt et à la diffusion de documents scientifiques de niveau recherche, publiés ou non, émanant des établissements d'enseignement et de recherche français ou étrangers, des laboratoires publics ou privés.

Graph Fourier Transform of fMRI temporal signals based on an averaged structural connectome for the classification of neuroimaging

Abdelbasset Brahim, Nicolas Farrugia

IMT Atlantique, Brest, France

Abstract

Graph signal processing (GSP) is a framework that enables the generalization of signal processing to multivariate signals described on graphs. In this paper, we present an approach based on Graph Fourier Transform (GFT) and machine learning for the analysis of resting-state functional magnetic resonance imaging (rs-fMRI). For each subject, we use rs-fMRI time series to compute several descriptive statistics in regions of interest (ROI). Next, these measures are considered as signals on an averaged structural graph built using tractography of the white matter of the brain, defined on the same ROI. GFT of these signals is computed using the structural graph as a support, and the obtained feature vectors are subsequently benchmarked in a supervised learning setting. Further analysis suggests that GFT using structural connectivity as a graph and the standard deviation of fMRI time series as signals leads to more accurate supervised classification using a world-wide multi-site database known as ABIDE (Autism Brain Imaging Data Exchange) when compared to several statistical metrics. Moreover, the proposed approach outperforms several approaches, based on using functional connectomes or complex functional network measures as features for classification.

Keywords: Graph Signal Processing, Machine Learning, Resting-State Analysis, Neuroimaging, Classification

1. Introduction

Functional magnetic resonance imaging (fMRI) is a noninvasive and safe imaging technique for measuring and mapping brain activity, and is commonly used in the field of cognitive neurosciences. However, the analysis of fMRI data is a major challenge due to a high sensitivity to noise, a large number of dimensions for few observations per subject, or different acquisition protocols [1]. Recently, there has been an increasing interest in the application of multivariate analysis and machine learning to understand complex properties of brain networks and to assist diagnosis in brain imaging data [2, 3]. However, few analysis approaches take into account both the multivariate aspect and the connectivity features of the brain, such as a structural graph estimated using white matter tractography, or functional connectivity graph computed using temporal covariation between neural activity time series.

As a potential answer to this challenges, Graph Signal Processing (GSP), which is an emerging sub-field of signal processing, takes into account the underlying graphical structure of multivariate data and aims to generalize classical signal processing techniques, such as filtering, convolution, or translation to irregular graph domains [4]. According to spectral graph theory [5], a Fourier transform can be defined on graphs from the eigendecomposition of the graph's Laplacian operator. Thus, GSP can be used to provide a spectral representation of signals defined on a graph, through the so-called Graph Fourier Transform operator (GFT). Therefore, GSP appears as an ideal framework to analyze fMRI data, as it enables to consider brain activity defined on a brain connectivity graph [6]. On the other hand, several statistical features, such as, the mean and the standard deviation (STD) of multivariate signals have previously been used to compute a vector with discriminatory (spatial) features for disease classification [7]. Thus, in this work, we evaluate a GSP-based approach for the analysis and the classification of neuroimaging data. We introduce a method based on resting state functional magnetic resonance imaging (rs-fMRI), consisting in measuring spontaneous brain activity of subjects at rest. Rs-fMRI is a very popular

method, due to the simplicity of its protocol, the wide availability of data and analysis methods, and the large body of evidence regarding its functional and clinical relevance [8, 9]. In our study, we assess whether the combination of an average structural graph with several statistical metrics on rs-fMRI signals
35 (such as STD) can extract meaningful features for the supervised classification of patients with autism spectrum disorder (ASD).

Related work: Several approaches for the classification of ASD patients using rs-fMRI have been proposed in the literature [3, 10–16]. Most approaches attempted to identify functional connectivity patterns that can discriminate patients from healthy subjects using rs-fMRI. In [3], the authors obtained pairwise
40 functional connectivity measurements from a lattice of 7266 regions of interest covering the gray matter for each subject. Then, a leave-one-out classifier was evaluated on these connections, which were grouped into multiple bins. An accuracy of 60% was obtained for whole brain classification using the Autism
45 Brain Imaging Data Exchange (ABIDE) datasets. In [10], authors presented a mathematical framework based on Riemannian geometry and kernel methods that can be applied to connectivity matrices for the classification of ASD. Their approach achieved an accuracy value of 60.76 %. however, it is validated on a small dataset of 79 subjects: 37 TC and 42 pathological subjects. In addition,
50 authors in [11], developed a diagnosis approach, in which, the correlation matrices computed from rs-fMRI time-series data, were considered as features and they were entered into a probabilistic neural network (PNN) classifier to separate ASD from TC. The correlation matrices of 640 subjects were classified as ASD or TC with approximately 90% accuracy using the PNN algorithm. Never-
55 theless, only subjects under 20 years of age were included in their study. In [12], authors proposed a diagnosis framework for ASD, which is based on the computation of Pearson correlation-based functional connectivity network of each cluster. The clusters are obtained by the decomposition of rs-fMRI time series into distinct clusters with similar spatial distribution of neural activity. Their
60 results achieved an accuracy rate of 71% and their framework was validated on several selected subjects from a subset of ABIDE database, i.e. the New York

University (NYU) Langone Medical Center. This dataset contains more than 170 subjects, however, the authors included only 92 selected subjects in their study. Moreover, authors in [13], investigated several pipelines that extract the most predictive biomarkers from the data by building participant-specific connectomes from functionally-defined brain areas. These connectomes are then compared across participants to learn patterns of connectivity that differentiate typical controls from ASD patients. The best pipeline lead to 67% prediction accuracy on the full ABIDE database. In [14], authors investigated patterns of functional connectivity that objectively identify ASD participants from rs-fMRI data using deep learning algorithms. Their results improved the state-of-the-art by achieving 70% accuracy in identification of ASD versus control patients in the ABIDE dataset. A novel metric learning method to evaluate distance between graphs that leverages the power of convolutional neural networks, while exploiting concepts from spectral graph theory to allow these operations on irregular graphs is proposed in [15]. The authors applied the proposed model to functional brain connectivity graphs from the ABIDE database. Their experimental results show that their method can learn a graph similarity metric tailored for a clinical application, improving the performance of a simple k -nn classifier by 11.9% compared to a traditional distance metric and a classification score of 62.9% was obtained for all the sites. In addition, authors in [16], introduced a new biomarker extraction pipeline for ASD that relies on the use of graph theoretical metrics of fMRI-based functional connectivity and machine learning algorithms. Their results suggest that measures of centrality provide the highest contribution to the classification power of a model for the >30 years age group, achieving an accuracy, sensitivity, and specificity of 95, 97, and 95%, respectively. However, their model is an age-dependent and in this age-range, there are only 51 subjects. Besides, the ABIDE dataset contains more than eight hundred subjects with a large age range (5 – 65).

Contributions: In this paper, we propose a novel multimodal analysis approach for brain imaging data, as shown in Figure 1. This analysis method combines GFT on a structural graph, and several statistical metrics of rs-fMRI

time series defined on the same brain regions than the structural graph, hence using two different imaging modalities : rs-fMRI and structural graph based
95 on white matter tractography. The proposed approach comprises four stages. Firstly, the Glasser atlas is used for brain parcellation [17] to extract the rs-fMRI time series of each subject. These time series are summarized by several statistical metrics, such as the temporal average or STD. Secondly, the resulting statistical measures are projected on an average structural graph of healthy sub-
100 jects from the Human Connectome Project (HCP) dataset using GFT. Then, in order to select the most informative features for classification, a univariate feature selection is performed using an analysis of variance (ANOVA). Finally, in order to keep the research finding more objective, two different classifiers are used to test the effectiveness of the proposed analysis method, namely a support
105 vector machine (SVM) with linear kernel and a logistic regression classifier.

The proposed approach provides a different insight from previous methods [3, 13–16], namely:

- The proposed method does not exploit functional connectivity matrices directly from rs-fMRI, but rather relies on descriptive statistics of time series, combined with spatial and anatomical information using mean struc-
110 tural connectivity of several healthy subjects and GFT;
- Our approach restores informative features related to neuro-psychiatric disease, such as ASD, as exemplified by statistically robust gains in clas- sification metrics when compared to other feature extraction methods, including functional connectivity and graph theoretical metrics;
115
- Taking into account the computational load, the proposed approach is less demanding when compared to functional connectomes-based approaches for the analysis of rs-fMRI brain data, as it is based only on the compu- tation of statistical metrics;
- The proposed approach decreases the amount of data needed to store
120 patient imaging data history, Thus, each subject can be defined by several

resulting features after their transformation using GFT defined on the same brain regions;

- Our method performs efficient dimensionality reduction, by using a statistical criterion to select the most predictive features.
- We extend our previous results on a small subset of ABIDE, i.e. NYU Langone Medical Center [18], showing that the proposed analysis framework performs well in the discrimination task between ASD and TC subjects, and outperforms most prior work on this subset.
- Finally, the proposed method is validated on a large world-wide multi-site database (ABIDE) in which different methods of imaging acquisition were used [19].

2. Materials and Methods

2.1. Database

The data used in this study were collected from the Autism Brain Imaging Data Exchange (ABIDE) datasets.¹ ABIDE I consists of 1112 subjects comprising 539 ASD patients and 573 Typical Controls (TC)[19]. For easy replication, this database has been preprocessed by the Configurable Pipeline for the Analysis of Connectomes (C-PAC) [20]. C-PAC uses several preprocessing techniques, such as, skull stripping, slice timing correction, motion correction, global mean intensity normalization, nuisance signal regression, band-pass filtering (0.01-0.1Hz) and registration of fMRI images to standard anatomical MNI space. The selection of the data is based on the results of quality visual inspection by three experienced clinicians who checked for largely incomplete brain coverage, high movement peaks, ghosting and other scanner artifacts. This yielded 871 subjects out of the initial 1112, consisting of 403 individuals suffering from ASD

¹See http://fcon_1000.projects.nitrc.org/indi/abide/abide_I.html for specific information.

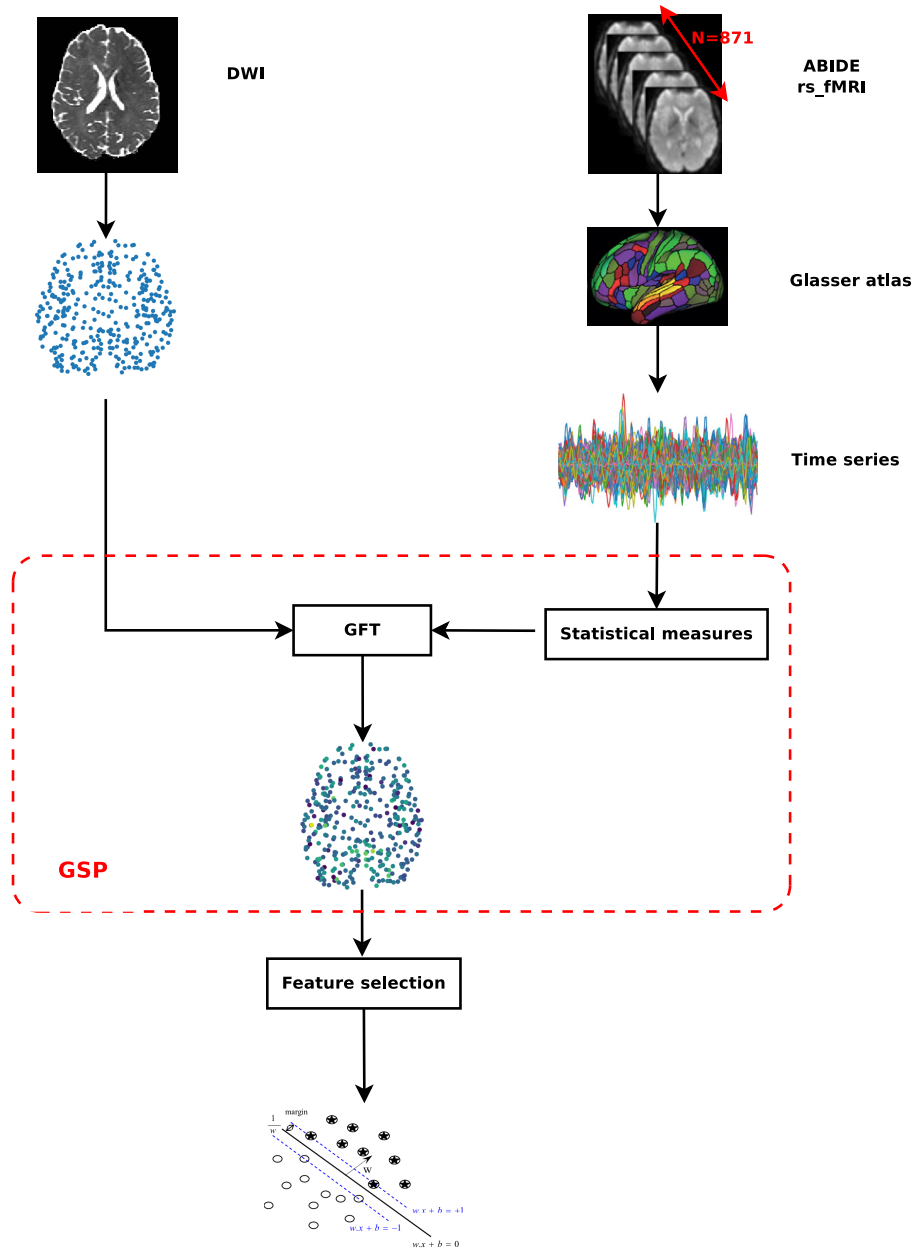


Figure 1: The graphical framework of the proposed approach.

and 468 TC. Due to the use of different acquisition protocols, the data is very different from one international site to another.

2.2. Regions of interest and Time-series extraction

150 The proposed approach is based, firstly, on regional time series extraction from brain parcellations. We used the Glasser parcellation [21], generated using multimodal data from the Human Connectome Project (HCP), totalizing in 360 regions. Thus, the time series of rs-fMRI brain imaging data were extracted according to 360 regions of interest (ROI) for each subject. Importantly, the
 155 same ROI are defined in the structural graph that is used to establish GFT.

2.3. Graph Signal Processing and Graph Fourier Transform on Structural Graph

In this work, we are interested in the analysis of rs-fMRI signals on an averaged structural graph. Let us first define an undirected, connected, weighted and symmetric graph $\mathcal{G} = \{\mathcal{V}, \mathcal{E}, \mathbf{W}\}$. The graph is characterized by a finite set of vertices \mathcal{V} indexed from 1 to N:

$$\mathcal{V} = \{v_1, \dots, v_N\} \quad (1)$$

as well as a set of edges \mathcal{E} in $\mathcal{V} \times \mathcal{V}$, and a weighted adjacency matrix \mathbf{W} , such that $\mathbf{W}_{ij} \in \mathbb{R}^+$ denotes the weight of the edge (v_i, v_j) .

The combinatorial graph Laplacian of a graph is defined by [6, 22]:

$$\mathbf{L} = \mathbf{D} - \mathbf{W} \quad (2)$$

where \mathbf{D} is the diagonal matrix of degrees defined by $\forall i : \mathbf{D}_{ii} = \sum_j \mathbf{W}_{ij}$.

Thus, the normalized Laplacian of graph is defined by [6]:

$$\mathbf{L}_n = \mathbf{D}^{-1/2} \mathbf{L} \mathbf{D}^{-1/2} \quad (3)$$

As \mathbf{L}_n is symmetric and real-valued matrix, it can be factorized using its eigenvectors as:

$$\mathbf{L}_n = \mathbf{V} \mathbf{\Lambda} \mathbf{V}^\top \quad (4)$$

where \mathbf{V} is the orthonormal matrix whose i th column is the eigenvector of \mathbf{L}_n , \mathbf{V}^\top is its transposed matrix, and \mathbf{A} is the diagonal matrix whose diagonal elements are the corresponding eigenvalues, such that $\mathbf{A}_{ii} = \lambda_i$ of \mathbf{L}_n .

In the context of GSP, we define signals \mathbf{x} as vectors in \mathbb{R}^N . The spectral representation of signals defined on the graph \mathcal{G} can be provided using GFT [4]:

$$\hat{\mathbf{x}} = \mathbf{V}^\top \mathbf{x} \quad (5)$$

Columns of \mathbf{V} can be interpreted as Fourier modes [4] and are relevant to describing signals with respect to typical propagation modes on the graph.

In this paper, we consider a graph whose nodes corresponding to 360 ROIs of
 160 the Glassers multimodal cortical atlas from HCP [21], with edges and weights are
 estimates of structural connectivity strength from several HCP healthy subjects,
 using white matter tractography techniques [23]. More precisely, the structural
 graph was obtained by averaging all subjects structural matrices. We defined
 GFT using the normalized Laplacian of this averaged structural graph. In the
 165 following sections, we setup a supervised classification task that compare several
 statistical measures that are subsequently transformed using GFT.

2.4. Feature extraction and Feature selection

We extracted several features with and without the use of GFT, based on
 descriptive statistics of the temporal rs-fMRI signals. Namely, we compared
 170 the STD, the mean, the variance and a high-order moment, i.e. the kurtosis
 of rs-fMRI time series. Next, we computed the projection of the same features
 on the structural graph of several healthy subjects in the graph Fourier domain
 using GFT. Moreover, for comparison purposes with the state of the art, we also
 extracted connectivity features via the covariance estimation of the tangent ma-
 175 trix [13, 24, 25], and we use the lower triangular part of the resulting functional
 connectivity (FC) matrix. Functional connectivity (FC) provides an index of the
 level of co-activation of brain regions based on the time-series of rs-fMRI brain
 imaging data. Finally, we also used the FC matrix to compute three complex

network measures known to be of interest in ASD research, namely eigenvec-
tor centrality (EC), node strength (NS) and clustering coefficient (CC) [16, 26].
180 These complex-graph network modeling approaches are seldom combined with
supervised learning. However, they could be relevant to identify brain sub-
systems associated with ASD [26]. Thus, we obtain a total of twelve feature
vectors, denoted by STD, STD+SG, Mean, Mean+SG, Var, Var+SG, Kurtosis,
185 Kurtosis+SG, FC, EC, NS and CC, respectively. These feature vectors are of
dimension N , except FC which is the size of the lower triangular connectivity
matrix, thus its size is $\frac{N(N-1)}{2}$ for each subject.

The main aim of this work is to present a novel modelling time series approach
applied on brain imaging. In order to validate the effectiveness and the robust-
ness of the proposed method in the analysis of rs-fMRI, we tested it on the
190 classification task for the diagnosis of ASD, basing on a widely used pipeline
for feature selection and for classification [13, 25]. Thus, in order to select the
best informative features and to remove non-informative features for classifi-
cation, univariate feature selection is performed by ANOVA. This technique is
195 based on the analysis of sample’s variance across the two categories. Features
that explain the largest proportion of the variance are retained. We tested the
selection from 10 up to 360 features with a *step* = 10 using this technique.

2.5. Cross-validation, classification and statistical analysis

We process the features selected by ANOVA in a cross-validated super-
vised classification setting using the most commonly used classifiers for these
200 datasets, i.e. l_2 -penalized support vector classification (SVC) with a linear ker-
nel ($C=0.01^2$) and l_2 -regularized logistic regression (LR) classifiers (solver=lbfgs³) [13,
25]. Different classification metrics, i.e. accuracy (Acc), sensitivity (Sen) and
specificity (Spe) are estimated using an *intra-site* cross-validation (CV) in or-
der to reduce the site-related variability. This CV scheme is based on stratified
205

²C is the penalty parameter of the error term

³lbfgs is the Broyden-Fletcher-Goldfarb-Shanno optimization algorithm

shuffle split cross-validation, which splits participants into training and test sets while preserving the ratio of samples for each site and condition. We used 80% of the participants for training and the remaining ones for testing. Importantly, feature selection was also performed within this cross-validated loop.

210 Finally, we performed robust statistical evaluations and comparisons between the different feature vectors to test whether the classifiers were able to predict significantly better than chance. We estimate the chance level of all trained classifiers using bootstrapping by calculating a permutation test score [27], i.e. repeating the classification procedure after randomizing the labels. This permutation test score provides an indication whether the trained classifier is likely
215 predicting at chance level.

2.6. Visualization of cross-validated selected features

We attempted to study qualitatively the stability and interpretability of the method, by visualizing feature selection with respect to cross-validation. We
220 calculated a vector of ratios that averages the number of times each feature is selected across folds. We then visualized these ratio back on the brain using the spatial extents of the ROI. In the case of features obtained using GFT, we applied the inverse GFT to the vector of ratios before visualization. The application of inverse GFT enables the visualization of the contribution of *all* regions
225 in the atlas, as opposed to the other features, for which only selected ROI are visualized.

3. Results and Discussion

3.1. Supervised Classification of ASD

230 ABIDE datasets are a heterogeneous data, which come from 17 international sites with no prior coordination, that is a typical clinical application setting. Thus, discriminating between ASD and TC individuals is a challenging task. Figures 2 and 3 reveal the averaged classification rates for the proposed method

across CV-folds, as a function of the number of features when compared to dif-
ferent statistical measures, FC and several complex network measures using LR
235 and SVC classifiers. The red markers, in the different approaches, reveals if the
classification metrics were statistically significant ($p < 0.01$) after a permutation
test using 100 permutations. The blue markers reveals the non significance of
the classification metrics for the different methods. Out of the different statis-
240 tical metrics, several of them turned out to yield non-significant classification
for all or most number of selected features, such as the mean of rs-fMRI. This
might be justified by the fact that there are relatively short time series included
in ABIDE datasets (typically 5-6 minutes per participant). However, features
with STD+SG yielded classifiers which are highly significantly above chance
245 level, even when selecting as few as 10 features.

Figure 4 shows the distribution of 100 classification scores obtained by permut-
ing labels, estimating true chance level and demonstrating that the observed
accuracy is highly significantly above chance level ($p < 0.01$). In the following
discussion, we will only consider approaches that lead to classifiers that are able
250 to predict better than chance level according to this permutation scheme.

Tables 1 and 2 show classification metrics for all methods that predicted bet-
ter than chance level. Interestingly, feature vectors with STD+SG outperform
those obtained using other statistical metrics, functional connectivity or several
complex-graph functional network modeling approaches.

255 Classification accuracies of 60.14% (55.92% for sensitivity, 67.77% for speci-
ficity, permutation test $p < 0.01$, 100 times) and 60.71% (56.30% for sensitivity,
68.03% for specificity, permutation test $p < 0.01$, 100 times) were achieved
by the STD+SG approach when the best 160 and 180 features are selected
(ANOVA) using LR and SVC classifiers. For instance, there is an accuracy
260 gain up to 4.4% and 4.31% using LR and SVC, respectively, when comparing
STD+SG approach with the remaining statistical methods and their projec-
tions. Moreover, comparing STD+SG with FC and several complex functional
network measures, there is an accuracy gain up to 5.95% and 6,46%, using the
different classifiers.

Approaches	Acc (%)	Sen (%)	Spe (%)
STD	57.68±0.044	55.74±0.047	77.76±0.052
STD+SG	60.14±0.035	55.92±0.046	67.77±0.042
Var	57.91±0.040	54.26±0.045	81.38±0.066
Var+SG	58.46±0.032	54.57±0.052	69.68±0.043
Kurtosis	57.22±0.033	44.56±0.064	87.55±0.080
Kurtosis+SG	55.74±0.029	35.92±0.062	87.82±0.044
FC	59.34±0.032	53.27±0.055	66.70±0.054
EC	56.40±0.030	49.01±0.058	66.06±0.048
NS	54.19±0.025	49.01±0.058	66.06±0.065
CC	56.91±0.040	52.53±0.041	68.77±0.054

Table 1: Maximum classification rates of the different approaches for ABIDE database using LR classifier (max ± STD).

265 Overall, the results of the present study suggest that a first-order statistical feature [7], such as the standard deviation of rs-fMRI time series extracted using Glasser parcellation may be a discriminating feature for the classification of a mental disorder like autism. In addition, projecting this statistical metric on the structural graph of a several healthy subject can help discriminate ASD
270 subjects from TC, as indicated by classification metrics. Thus, these findings suggest that a multimodal neuroimaging approach may lead to greater accuracy than a single modality, such as functional connectome alone.

Furthermore, it is worth noting that the proposed approach is different from previous methods [3, 13–16] in the classification of autism using rs-fMRI, in which
275 the most popular approach is to exploit the whole functional connectivity matrix in the framework of functional connectome-based classification pipeline.

3.2. Comparison with the state of the art

The proposed rs-fMRI analysis method was compared with several approaches for an ASD diagnosis from the literature, as shown in Tables 3 and 4. The com-

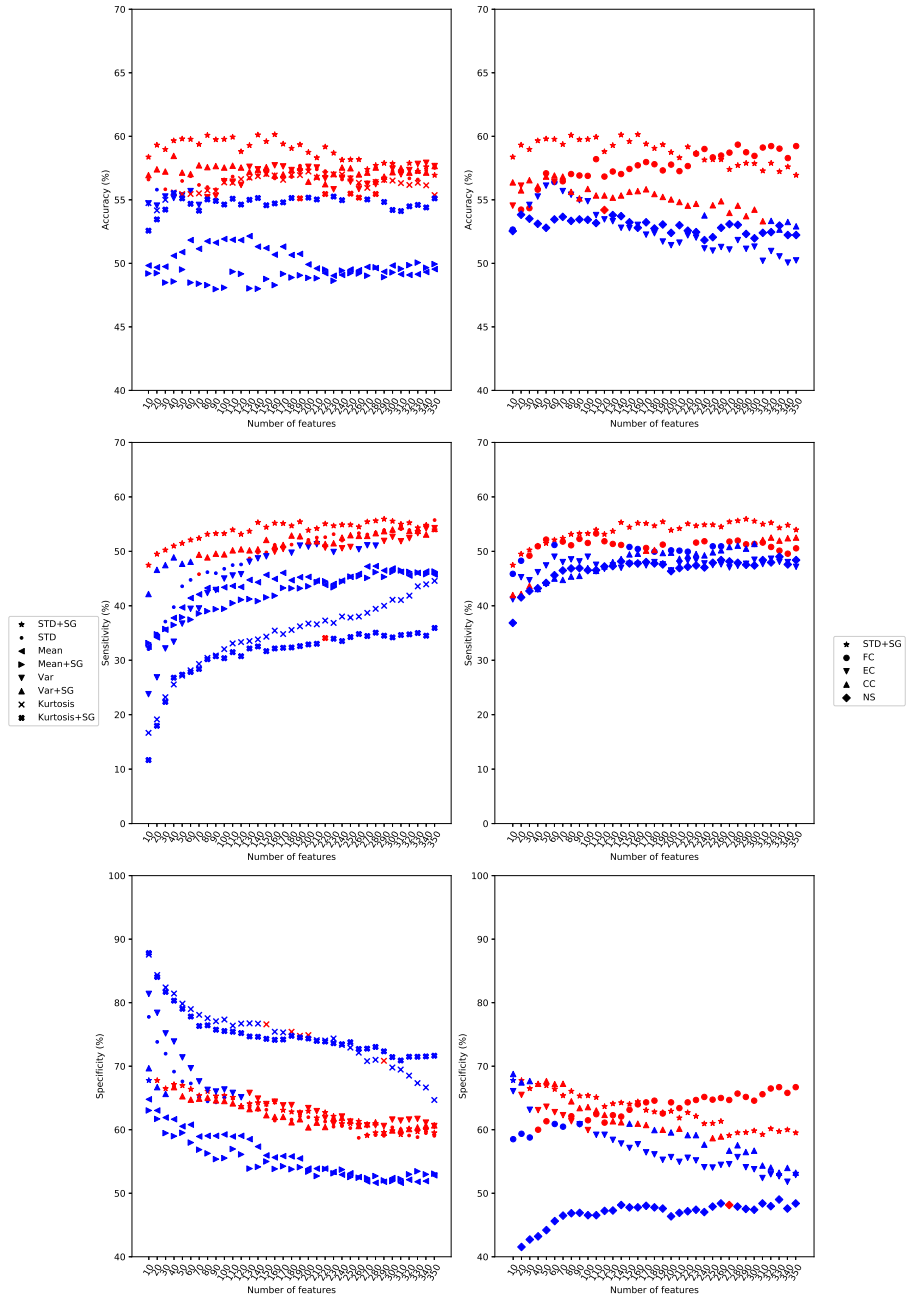


Figure 2: Left: Average accuracy, sensitivity and specificity across 20 CV-folds, as a function of number of features and statistical approaches using LR classifier. Right: Average accuracy, sensitivity and specificity across 20 CV-folds, as a function of number of features when compared to FC and complex network measures approaches using LR classifier. Red (resp. blue) markers indicate classification significantly above chance level (resp. no better than chance) .

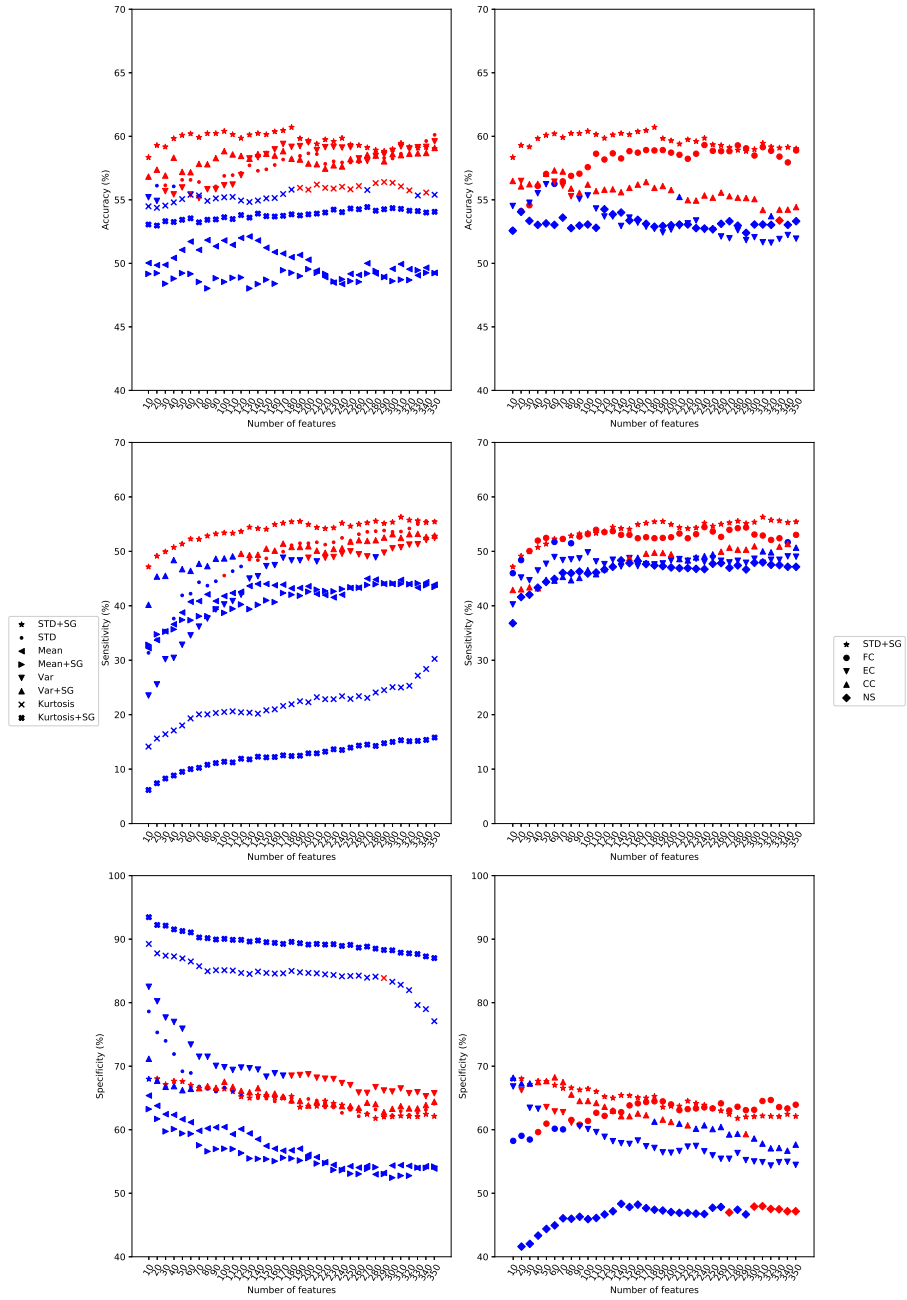


Figure 3: Left: Average accuracy, sensitivity and specificity across 20 CV-folds, as a function of number of features and statistical approaches using SVC classifier. Right: Average accuracy, sensitivity and specificity across 20 CV-folds, as a function of number of features when compared to FC and complex network measures approaches using SVC classifier. Red (resp. blue) markers indicate classification significantly above chance level (resp. no better than chance) .

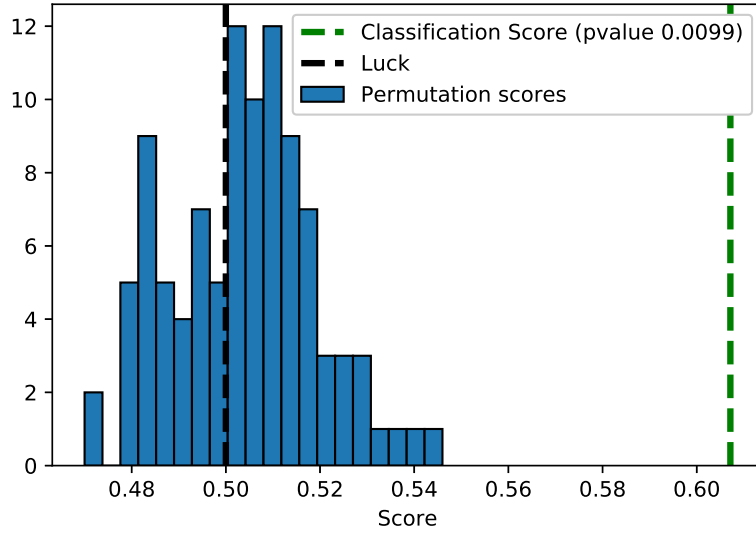


Figure 4: Permutation scores of the STD+SG approach and observed classification score (accuracy), using 100 permutations for 180 best selected feature using ANOVA.

Approaches	Acc (%)	Sen (%)	Spe (%)
STD	60.11±0.033	55.55±0.041	78.61±0.047
STD+SG	60.71±0.034	56.30±0.051	68.03±0.046
Var	59.60±0.037	52.47±0.038	82.50±0.066
Var+SG	59.09±0.034	53.21±0.047	71.17±0.044
Kurtosis	56.4±0.021	30.25±0.069	89.25±0.076
FC	59.31±0.040	54.44±0.045	64.68±0.049
EC	56.48±0.026	49.81±0.052	66.81±0.049
NS	54.25±0.029	48.33±0.044	48.33±0.044
CC	57.31±0.038	51.35±0.047	68.24±0.048

Table 2: Maximum classification rates of the different approaches for ABIDE database using SVC classifier with linear kernel (max ± STD).

280 parison is based on three criteria, i.e. the number of subjects, number of features
used for the classification and the resulting accuracy values. Taking into account
more than 870 subjects from ABIDE database, the proposed approach might
be comparable with the studies in [3, 13, 15], although, we did not use the
optimal pipeline for feature selection and classification. These differences in
285 feature selection/classification algorithms might account for the differences in
classification accuracy between the studies. However, in the studies [11], only
subjects under 20 years of age were included in their study and their model is
an age-dependent.

Moreover, when using the biggest subset from the full ABIDE, such as the data
290 from the NYU Langone Medical Center site only [18], the proposed approach
outperforms the state of the art methods, such as in [3, 10, 14]. Specifically,
when comparing to [14], our proposed method is able to outperform recent
methods based on more fashionable techniques such as deep learning applied
on hundreds of subjects. The slight difference in the accuracy value with [12],
295 may be justified by the difference in the number of subjects for the same NYU
dataset. Thus, these results were required to be validated in the whole dataset
using all samples.

However, it should be noted that the accuracy value of the multisite sample, i.e.
the whole ABIDE database was smaller than for the monosite sample, i.e. NYU
300 dataset. This can be justified by several factors, such as the heterogeneities
in scanning protocols, called site effects, imaging sequences, acquisition param-
eters, and subject populations [28]. Such heterogeneities will definitely limit
the sensitivity for detecting abnormalities induced by ASD, resulting in a drop
in accuracy value from monosite to multisite data. This commonly motivates
305 researchers to limit the number of sites included in their analyses at the cost of
sample size.

In a nutshell, these tables reveal the reproducibility and generalizability of our
proposed framework, which may work on small and even big databases, as exem-
plified by statistically robust gains in the classification metrics. However, from
310 a methodological point of view, our main aim of this study is to present a novel

Approach	N. of subjects	N. of features	Accuracy (%)
STD+SG with SVC	871	180	60.71
Nielsen et al. 2013 [3]	964	7266	60
Iidaka et al. 2015 [11]	640	90	90
Ira Ktena et al. 2017 [15]	871	128	62.9
Abraham et al. 2017 [13]	871	84	66.9

Table 3: Comparison of different approaches for classification of the ABIDE database.

Approach	N. of subjects	N. of features	Accuracy (%)
STD+SG with SVC [18]	172	100	70.36
Nielsen et al. 2013 [3]	179	7266	65
Dodero et al. 2015 [10]	79	264	60.76
Wee et al. 2016 [12]	92	116	71
Heinsfeld et al. 2018 [14]	175	19,900	66

Table 4: Comparison of different approaches for classification of a subset of the ABIDE dataset.

modelling time series approach applied on rs-fMRI brain imaging, nor the identification of biomarkers for ASD using intrinsic functional brain connectivity, as in [3, 10–16]. Moreover, the analytic procedure employed in the present study represents an entirely hypothesis-free, GSP-based approach and we provide our analysis code for replicability (see section Data and Code Availability).

3.3. Visualizations of features

Figure 5 depicts a visualization of 50 best features selected with ANOVA, averaged over folds. Using features from CC, STD and Var, many ROIs are consistently selected across folds as indicated by ratios close to 1, for example the left inferior temporal cortices, right anterior and posterior cingulate cortices. Notably, the spatial reconstruction of selected features in the graph Fourier domain, estimated using inverse GFT, reveals whole brain patterns that involve

all 360 ROIs. These patterns are similar for $STD+SG$ and $Var+SG$, and partly overlap with the spatial locations of ratios obtained with the other features
 325 (e.g. left inferior temporal cortex), while adding other ROIs such as the left and right precentral gyri. These regions may be relevant for diagnosis of ASD, as reported in previous studies [12, 13]. This visualization provides qualitative evidence that the accuracy boost obtained using GFT might be explained by the efficient combination of whole brain patterns with only a fraction of features,
 330 which results in an efficient feature selection strategy.

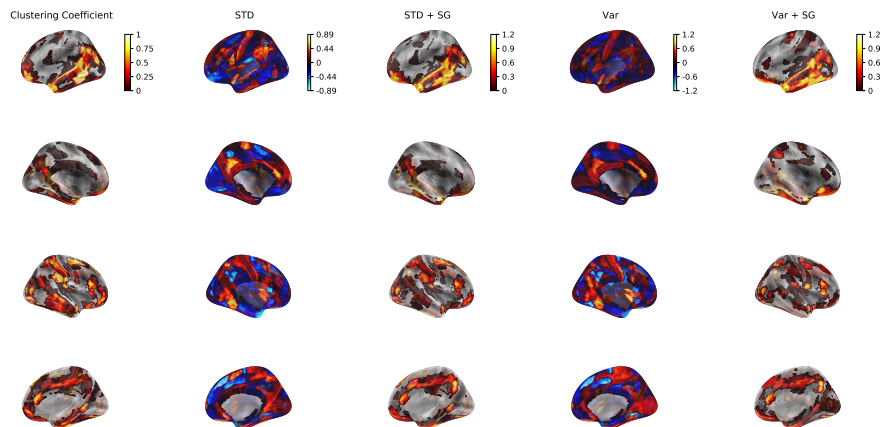


Figure 5: Spatial distributions of ratios (%) (respectively inverse GFT of ratios for $STD+SG$ and $Var+SG$) over 20 folds of the 50 best selected features using ANOVA. Rows correspond to different views of the cortical surface, namely left lateral, left medial, right lateral and right medial views.

3.4. Limitations and future directions

The main limitation of this study work is probably that we focus only on Glasser brain parcellations, which is generated using multimodal data, to extract regional time series and to build the structural graph. In future studies,
 335 analyses using another kind of parcellations may be of interest and should be compared to replicate the accuracy of classification, as the choice of parcellation has previously been benchmarked as an important source of variability for classification [13].

Besides, while we used the most popular methods for classification in this
340 database, it is likely that its findings regarding optimal pipeline decisions will
carry over to other aggregate samples, as well as more homogeneous samples.
Future studies may wish to validate this point, by extending this approach to
larger and more homogeneous samples. Moreover, as one obvious source of
heterogeneity in ASD is the gender [29], the results may be disproportionately
345 skewed. Thus, future research should take into consideration this confound-
ing variable to reduce the effects of heterogeneity for improving classification
performances.

Another limitation of our work is the fact that we computed graph signals
from time series using the standard deviation, but the resulting signal to noise
350 ratio is sensitive to the length of the time series. As a consequence, a promising
direction would be to address this issue by considering other statistical esti-
mates.

Next, we limited our experiments to straightforward supervised learning
methods with few parameters, namely support vector machines and logistic
355 regression. Recent development in machine learning have witnessed spectacular
progress due to deep learning architectures, which are based on a much larger
number of parameters. While other authors have proposed deep learning based
approaches to classify ASD [14], we suggest that the approach proposed in the
current paper could be combined with deep learning on graphs [30], as our
360 method already extracts relevant features by exploiting the graphs using GFT.

4. Conclusion

In the current study, we present a novel and efficient approach for the analy-
sis of rs-fMRI. More specifically, this work has introduced the application of GSP
on several descriptive statistics, such as the temporal variability of rs-fMRI. In
365 order to validate the effectiveness and the robustness of the proposed method,
we tested its ability in distinguishing between healthy and ASD patients. Fur-
ther analysis demonstrated that this multimodal analysis approach can improve

the classification performances, despite needing few parameters. Thus, the general trend of our findings reveals that the analysis of rs-fMRI data may not
370 mainly based on brain functional connectomes approaches, while incorporating structural connectivity together with temporal variability may result in a gain in predictive power.

Data and code availability

We share the resulting time-series from Glasser atlas and the scripts to re-
375 produce the classification results and the visualizations in: <https://github.com/AbdelbassetBrahim/GSP-applied-on-ASD-classification>. For the implementation of the different machine learning methods in this paper, we rely on efficient implementations open-source scientific computing packages using Python 3.7. For classification, cross-validation and selection methods, we rely
380 on the scikit-learn library [31] v0.20.1. For downloading the dataset, building the connectivity measures and brain visualization, we use Nilearn v0.5.2 [32], while matplotlib is used for generating other figures. Finally, all graph signal processing was done using pygsp package v0.5.1.

Acknowledgments

385 The research was partly supported by the Bretagne region, under the framework "Stratégie d'Attractivité Durable" within the project "Traitement du Signal sur Graphes". We wish to thank Maria Giulia Pretti and Dimitri Van De Ville for sharing their average structural graph.

References

- 390 [1] G. Varoquaux, B. Thirion, How machine learning is shaping cognitive neuroimaging, *GigaScience* 3 (1) (2014) 28.
- [2] D. S. Bassett, O. Sporns, *Network neuroscience*, Vol. 20(3), 2017.

- [3] J. A. Nielsen, B. A. Zielinski, P. T. Fletcher, A. L. Alexander, N. Lange, E. D. Bigler, J. E. Lainhart, J. S. Anderson, Multisite functional connectivity mri classification of autism: Abide results, *Front Hum Neurosci* 7(599).
395
- [4] D. I. Shuman, S. K. Narang, P. Frossard, A. Ortega, P. Vandergheynst, The emerging field of signal processing on graphs: Extending high-dimensional data analysis to networks and other irregular domains, *IEEE Signal Processing Magazine* 30 (3) (2013) 83–98.
- [5] F. R. Chung, *Spectral graph theory*, Vol. 92, 1997.
400
- [6] W. Huang, T. A. W. Bolton, J. D. Medaglia, D. S. Bassett, A. Ribeiro, D. V. D. Ville, A graph signal processing perspective on functional brain imaging, *Proceedings of the IEEE* 106 (5) (2018) 868–885.
- [7] A. Singh, M. K. Dutta, R. Jennane, E. Lespessailles, Classification of the trabecular bone structure of osteoporotic patients using machine vision,
405 *Computers in Biology and Medicine* 91 (2017) 148158.
- [8] S. M. Smith, D. Vidaurre, C. F. Beckmann, M. F. Glasser, M. Jenkinson, K. L. Miller, T. E. Nichols, E. C. Robinson, G. Salimi-Khorshidi, M. W. Woolrich, et al., Functional connectomics from resting-state fmri, *Trends*
410 *in cognitive sciences* 17 (12) (2013) 666–682.
- [9] M. D. Fox, M. Greicius, Clinical applications of resting state functional connectivity, *Frontiers in systems neuroscience* 4 (2010) 19.
- [10] L. Dodero, H. Q. Minh, M. San Biagio, V. Murino, D. Sona, Kernel-based classification for brain connectivity graphs on the riemannian manifold of
415 positive definite matrices, in: *2015 IEEE 12th International Symposium on Biomedical Imaging (ISBI)*, IEEE, 2015, pp. 42–45.
- [11] T. Iidaka, Resting state functional magnetic resonance imaging and neural network classified autism and control, *Cortex* 63 (2015) 55–67.

- [12] C.-Y. Wee, P.-T. Yap, D. Shen, Diagnosis of autism spectrum disorders using temporally distinct resting-state functional connectivity networks, *CNS neuroscience & therapeutics* 22 (3) (2016) 212–219.
- [13] A. Abraham, M. P. Milham, A. D. Martino, R. C. Craddock, D. Samaras, B. Thirion, G. Varoquaux, Deriving reproducible biomarkers from multi-site resting-state data: An autism-based example, *NeuroImage* 147 (2017) 736 – 745.
- [14] A. S. Heinsfeld, A. R. Franco, R. C. Craddock, A. Buchweitz, F. Meneguzzi, Identification of autism spectrum disorder using deep learning and the abide dataset, *NeuroImage. Clinical* 17 (2018) 16–23.
- [15] S. I. Ktena, S. Parisot, E. Ferrante, M. Rajchl, M. C. H. Lee, B. Glocker, D. Rueckert, Distance metric learning using graph convolutional networks: Application to functional brain networks, in: *International Conference on Medical Image Computing and Computer-Assisted Intervention*, Vol. abs/1703.02161, 2017. [arXiv:1703.02161](https://arxiv.org/abs/1703.02161).
- [16] A. Kazeminejad, R. C. Sotero, Topological properties of resting-state fmri functional networks improve machine learning-based autism classification, *Frontiers in Neuroscience* 12 (2019) 1018.
- [17] M. F. Glasser, T. S. Coalson, E. C. Robinson, C. D. Hacker, J. Harwell, E. Yacoub, K. Ugurbil, J. Andersson, C. F. Beckmann, M. Jenkinson, et al., A multi-modal parcellation of human cerebral cortex, *Nature* 536 (7615) (2016) 171.
- [18] A. Brahim, M. Hajjam El Hassani, N. Farrugia, Classification of autism spectrum disorder through the graph fourier transform of fmri temporal signals projected on structural connectome, in: M. Vento, G. Percannella, S. Colantonio, D. Giorgi, B. J. Matuszewski, H. Kerdegari, M. Razaak (Eds.), *Computer Analysis of Images and Patterns*, Springer International Publishing, Cham, 2019, pp. 45–55.

- [19] A. Di Martino, C. G. Yan, Q. Li, E. Denio, F. X. Castellanos, K. Alaerts, J. S. Anderson, M. Assaf, S. Y. Bookheimer, M. Dapretto, B. Deen, S. Delmonte, I. Dinstein, B. Ertl-Wagner, D. A. Fair, L. Gallagher, D. P. Kennedy, C. L. Keown, C. Keysers, J. E. Lainhart, C. Lord, B. Luna, V. Menon, N. J. Minshew, C. S. Monk, S. Mueller, R. A. Mller, M. B. Nebel, J. T. Nigg, K. O’Hearn, K. A. Pelphrey, S. J. Peltier, J. D. Rudie, S. Sunaert, M. Thioux, J. M. Tyszka, L. Q. Uddin, J. S. Verhoeven, N. Wenderoth, J. L. Wiggins, S. H. Mostofsky, M. P. Milham, The autism brain imaging data exchange: towards a large-scale evaluation of the intrinsic brain architecture in autism., *Mol Psychiatry* 19(6) (2014) 659–67.
- [20] C. Craddock, S. Sikka, B. Cheung, R. Khanuja, S. S. Ghosh, C. Yan, Q. Li, D. Lurie, J. Vogelstein, R. Burns, S. Colcombe, M. Mennes, C. Kelly, A. Di Martino, F. X. Castellanos, M. Milham, Towards automated analysis of connectomes: The configurable pipeline for the analysis of connectomes (c-pac), *Frontiers in Neuroinformatics* (42).
- [21] M. F. Glasser, T. S. Coalson, E. C. Robinson, C. D. Hacker, J. Harwell, E. Yacoub, K. Ugurbil, J. Andersson, C. F. Beckmann, S. S. M. Jenkinson, M., D. C. Van Essen, A multi-modal parcellation of human cerebral cortex, *Nature* vol. 536,7615 (2016): 171-178. 536 (7615) (2016) 171–178.
- [22] W. Huang, L. Goldsberry, N. F. Wymbs, S. T. Grafton, D. S. Bassett, A. Ribeiro, Graph frequency analysis of brain signals, *IEEE Journal of Selected Topics in Signal Processing* 10 (7) (2016) 1189–1203.
- [23] M. G. Preti, D. V. D. Ville, Decoupling of brain function from structure reveals regional behavioral specialization in humans [arXiv:1905.07813v1](https://arxiv.org/abs/1905.07813v1).
- [24] G. Varoquaux, F. Baronnet, A. Kleinschmidt, P. Fillard, B. Thirion, Detection of brain functional-connectivity difference in post-stroke patients using group-level covariance modeling, in: *Medical Image Computing and Computer-Assisted Intervention*, 2010.

- 475 [25] K. Dadi, M. Rahim, A. Abraham, D. Chyzyk, M. Milham, B. Thirion,
G. Varoquaux, Benchmarking functional connectome-based predictive
models for resting-state fmri, *NeuroImage* 192 (2019) 115 – 134.
- [26] J. R. Sato, C. V. M., S. de Siqueira Santos, K. Brauer Massirer, A. Fu-
jita, Complex network measures in autism spectrum disorders, *IEEE/ACM*
480 *Trans Comput Biol Bioinform* 15(2) (2018) 581–587.
- [27] P. Golland, B. Fischl, Permutation tests for classification: towards sta-
tistical significance in image-based studies, in: *Information processing in*
medical imaging, 2003, pp. 330–341.
- [28] C. Dansereau, Y. Benhajali, C. Risterucci, E. M. Pich, P. Orban,
485 D. Arnold, P. Bellec, Statistical power and prediction accuracy in mul-
tisite resting-state fmri connectivity, *NeuroImage* 149 (2017) 220 – 232.
doi:<https://doi.org/10.1016/j.neuroimage.2017.01.072>.
URL [http://www.sciencedirect.com/science/article/pii/
S1053811917300939](http://www.sciencedirect.com/science/article/pii/S1053811917300939)
- 490 [29] M. C. Lai, M. V. Lombardo, J. Suckling, A. N. Ruigrok, B. Chakrabarti,
C. Ecker, S. Deoni, M. Craig, D. Murphy, E. Bullmore, M. A. Consortium,
S. Baron-Cohen, Biological sex affects the neurobiology of autism, *Brain :
a journal of neurology* 136(9) (2013) 2799–2815.
- [30] Z. Wu, S. Pan, F. Chen, G. Long, C. Zhang, P. S. Yu, A comprehensive
495 survey on graph neural networks, arXiv preprint arXiv:1901.00596.
- [31] F. Pedregosa, G. Varoquaux, A. Gramfort, V. Michel, B. Thirion, O. Grisel,
M. Blondel, P. Prettenhofer, R. Weiss, V. Dubourg, J. Vanderplas, A. Pas-
sos, D. Cournapeau, M. Brucher, M. Perrot, E. Duchesnay, Scikit-learn:
Machine learning in python, *J. Mach. Learn. Res.* 12 (2011) 2825–2830.
500 URL <http://dl.acm.org/citation.cfm?id=1953048.2078195>
- [32] A. Abraham, F. Pedregosa, M. Eickenberg, P. Gervais, A. Mueller, J. Kos-
saifi, A. Gramfort, B. Thirion, G. Varoquaux, Machine learning for neu-

roimaging with scikit-learn, *Frontiers in Neuroinformatics* 8 (2014) 14.
doi:10.3389/fninf.2014.00014.